

# Unprecedented Synthesis of 1,3-Dimethylcyclobutadiene in the Solid State and Aqueous Solution

Yves-Marie Legrand, Arnaud Gilles, Eddy Petit, Arie van der Lee, and Mihail Barboiu\*<sup>[a]</sup>

**Abstract:** Cyclobutadiene (CBD), the smallest cyclic hydrocarbon bearing conjugated double bonds, has long intrigued chemists because of its chemical characteristics. The question of whether the molecule could be prepared at all has been answered, but the parent compound and its unperturbed derivatives have eluded crystallographic characterization or synthesis “in water”. Different approaches have been used to generate and to trap cyclobutadiene in a variety of confined environments: a) an Ar matrix at cryogenic temperatures, b) a hemicarcerand cage enabling the characterization by NMR spectroscopy in solution, and c) a crystalline guanidinium–sulfonate–calixarene **G<sub>4</sub>C** matrix that is stable enough to allow photoreactions in the

solid state. In the latter case, the 4,6-dimethyl- $\alpha$ -pyrone precursor, **Me<sub>2</sub>1**, has been immobilized in a guanidinium–sulfonate–calixarene **G<sub>4</sub>C** crystalline network through a combination of non-covalent interactions. UV irradiation of the crystals transforms the entrapped **Me<sub>2</sub>1** into a 4,6-dimethyl-Dewar- $\beta$ -lactone intermediate, **Me<sub>2</sub>2**, and rectangular-bent 1,3-dimethylcyclobutadiene, **Me<sub>2</sub>CBD<sup>R</sup>**, which are sufficiently stable under the confined conditions at 175 K to allow a conventional structure determination by X-ray diffraction. Further irradiation drives the reaction towards

**Keywords:** calixarene • cyclobutadiene • Dewar- $\beta$ -lactone • host–guest systems • X-ray diffraction

**Me<sub>2</sub>3&Me<sub>2</sub>CBD<sup>S</sup>/CO<sub>2</sub>** (63.7%) and **Me<sub>2</sub>CBD<sup>R</sup>** (37.3%) superposed crystalline architectures and the amplification of **Me<sub>2</sub>CBD<sup>R</sup>**. The crystallographic models are supported by additional FTIR and Raman experiments in the solid state and by <sup>1</sup>H NMR spectroscopy and ESI mass spectrometry experiments in aqueous solution. Amazingly, the 4,6-dimethyl-Dewar- $\beta$ -lactone, **Me<sub>2</sub>2**, the cyclobutadiene-carboxyl zwitterion, **Me<sub>2</sub>3**, and 1,3-dimethylcyclobutadiene, **Me<sub>2</sub>CBD**, were obtained by ultraviolet irradiation of an aqueous solution of **G<sub>4</sub>C{Me<sub>2</sub>1}**. 1,3-Dimethylcyclobutadiene is stable in water at room temperature for several weeks and even up to 50 °C as demonstrated by <sup>1</sup>H NMR spectroscopy.

## Introduction

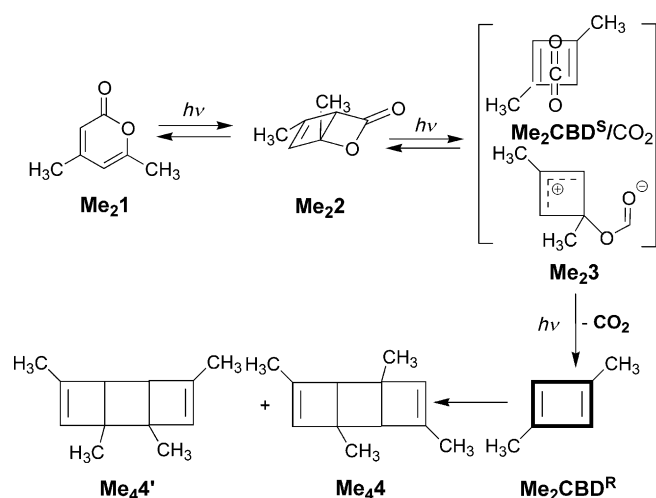
The chemistry of cyclobutadiene (CBD)<sup>[1–8]</sup> and the corresponding theoretical calculations<sup>[9–14]</sup> have been the object of significant research effort. Crucial experiments leading to trapping cyclobutadiene and to understanding its properties and to elucidating its structure have provided a number of highlights over the last 40 years. The Ar matrix isolation of cyclobutadiene by Corey,<sup>[1]</sup> Chapman,<sup>[2]</sup> Krantz,<sup>[3,4]</sup> Maier,<sup>[5–7]</sup> Michl<sup>[8]</sup> and their respective co-workers are non-exclusive examples of the fascinating facets of cyclobutadiene chemistry.<sup>[5–7]</sup> In a seminal experiment Cram and co-workers succeeded in isolating cyclobutadiene by sequestering it in a hemicarcerand cage in solution, thereby inhibiting

its dimerization.<sup>[15,16]</sup> The question of whether the molecule could be prepared at all was largely answered, but cyclobutadiene and its unperturbed precursors have eluded crystallographic characterization. A further successful approach is related to the design of a crystalline host matrix that might present: a) good quality diffraction data and b) an optimal design of the host confining volume, dimensionally adapted to the cyclobutadiene precursor guests and/or presenting anchoring fixing groups. These considerations inspired us to design an appropriate crystalline host matrix for the synthesis of cyclobutadiene. The photolysis reaction of the 4,6-dimethyl- $\alpha$ -pyrone precursor **Me<sub>2</sub>1** under confinement in a protective guanidinium–calixarene–sulfonate **G<sub>4</sub>C** matrix allows the preparation of the dimethyl-Dewar- $\beta$ -lactone **Me<sub>2</sub>2**, the 1,3-cyclobutadiene-carboxyl zwitterion intermediate **Me<sub>2</sub>3**, as well as 1,3-dimethylcyclobutadiene, **Me<sub>2</sub>CBD**, in the solid crystalline state and in aqueous solution (Scheme 1).<sup>[17,18]</sup> We report here a more detailed analysis of the formation of **Me<sub>2</sub>CBD** in the solid state, based on more advanced refinements of the original X-ray data and on new supporting FTIR, Raman, and NMR spectroscopic, and ESI mass spectrometric data. 1,3-Dimethylcyclobutadiene is stable in water in the presence of the **G<sub>4</sub>C** matrix at room

[a] Dr. Y.-M. Legrand, Dr. A. Gilles, E. Petit, Dr. A. van der Lee, Dr. M. Barboiu

Adaptive Supramolecular Nanosystems Group  
Institut Européen des Membranes  
ENSCM-UMI-UMR-CNRS5635  
Place Eugène Bataillon CC047  
34095 Montpellier Cedex 5 (France)  
E-mail: mihai.barboiu@iemm.univ-montp2.fr

Supporting information for this article is available on the WWW under <http://dx.doi.org/10.1002/chem.201100693>.



Scheme 1. Electrocyclic rearrangement under confined conditions in aqueous solution of  $\alpha$ -pyrone **Me<sub>2</sub>1** leads to 4,6-dimethyl-Dewar- $\beta$ -lactone, **Me<sub>2</sub>2**; photo-fragmentation of **Me<sub>2</sub>2** occurs via the 1,3-cyclobutadiene-carboxylate zwitterion **Me<sub>2</sub>3** or **Me<sub>2</sub>CBD<sup>S</sup>/CO<sub>2</sub>** complex, which, by eliminating CO<sub>2</sub>, leads to 1,3-dimethylcyclobutadiene, **Me<sub>2</sub>CBD<sup>R</sup>**. Finally, conversion of **Me<sub>2</sub>CBD<sup>R</sup>** leads to its dimers **Me<sub>2</sub>4** and **Me<sub>2</sub>4'**.

temperature for several weeks and even up to 50 °C during the NMR measurements.

## Results and Discussion

### Solid-state photosynthesis of CBD in a crystalline matrix under confined conditions:

Inclusion of 4,6-dimethyl- $\alpha$ -pyrone, **Me<sub>2</sub>1**, within the **G<sub>4</sub>C** matrix<sup>[17–19]</sup> in an aqueous solution of either **G<sub>4</sub>C/Me<sub>2</sub>1** or **4·G/C/Me<sub>2</sub>1** components led to single crystals of **G<sub>4</sub>C{Me<sub>2</sub>1}** (Figure 1).

The structural contributions of **G** to the **G<sub>4</sub>C{Me<sub>2</sub>1}** architecture are: a) stabilization through hydrogen bonding of the cone conformation of the calixarene **C**, in which the 4-Me group of **Me<sub>2</sub>1** is fixed through three CH- $\pi$  interactions;<sup>[20]</sup> b) sandwiching of the fully localized canonical form<sup>[21]</sup> of **Me<sub>2</sub>1** between two **G** groups while c) the carbonyl oxygen atom of **Me<sub>2</sub>1** points outward, forming anchoring hydrogen bonds with a third quasi-coplanar **G** cation (Figure 1) (see the Supporting Information for details).<sup>[17]</sup>

Importantly, during the irradiation of **G<sub>4</sub>C{Me<sub>2</sub>1}**, the **G<sub>4</sub>C** matrix remains unchanged (Figure 2a), whereas the structure of confined **Me<sub>2</sub>1** is modified during the series of irradiations (Figure 2b). Such irradiation procedures (2 × 10 min) induce the conversion of **G<sub>4</sub>C{Me<sub>2</sub>1}** into the **G<sub>4</sub>C{Me<sub>2</sub>1&Me<sub>2</sub>2&Me<sub>2</sub>CBD<sup>R</sup>}** architecture (Figure 3). The cigar-shaped ellipsoid for atom C3 led us to use a two-way split model for C3, consistent with the co-existence of a distorted **Me<sub>2</sub>1** geometry and the ‘butterfly’-type geometry of **Me<sub>2</sub>2** (Figure 3).<sup>[14]</sup> Supplementary separate density maxima on the electronic density map were detected on both sides of **Me<sub>2</sub>2**, corresponding to 22.7% conversion of **Me<sub>2</sub>2** to **Me<sub>2</sub>CBD<sup>R</sup>**. They remain stable after the splitting model was applied (Figure 3).

The **Me<sub>2</sub>CBD<sup>R</sup>** ring shows a relaxed rectangular-bent geometry, asymmetrically distorted, its plane being slightly flipped with the methyl groups lying out-of-plane with similar bond lengths and angles as predicted by theory<sup>[22,23]</sup> and experiments for the ground state of **Me<sub>2</sub>CBD<sup>R</sup>**.<sup>[24–26]</sup> Further irradiation (60 min) led to the transformation of both **Me<sub>2</sub>1** and **Me<sub>2</sub>2** into superposed **Me<sub>2</sub>3&Me<sub>2</sub>CBD<sup>S</sup>/CO<sub>2</sub>** structures

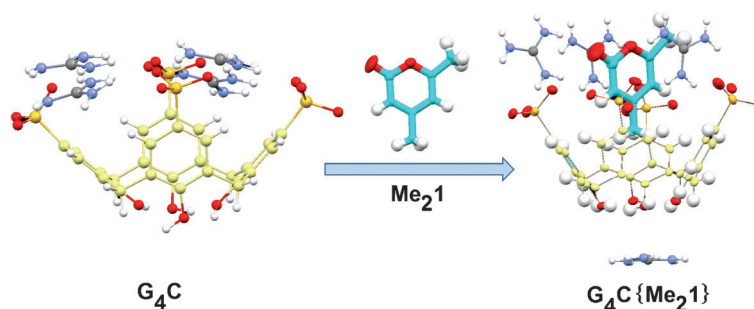


Figure 1. Crystal structures of the **G<sub>4</sub>C** host matrix and of the **G<sub>4</sub>C{Me<sub>2</sub>1}** host-guest complex.<sup>[17]</sup>

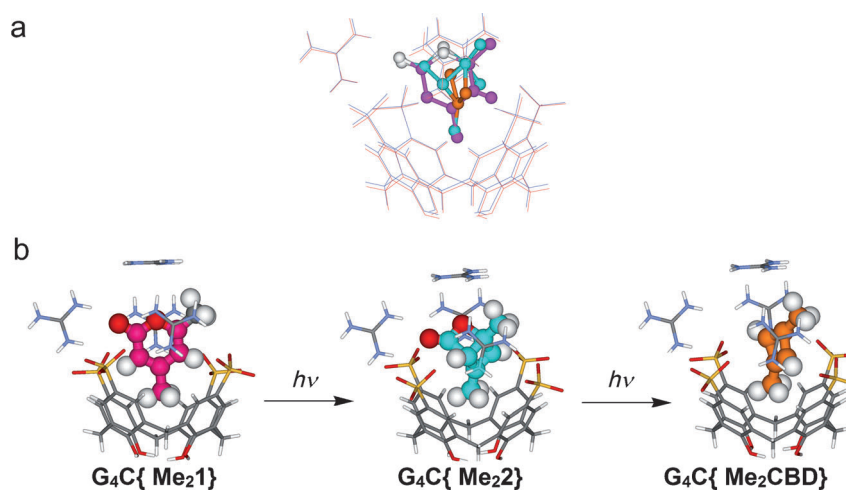


Figure 2. X-ray crystallographic representation of the **Me<sub>2</sub>CBD** formation pathway from photolysis of **Me<sub>2</sub>1**: a) Views of the initial (red line) and irradiated (blue line) single-crystal X-ray structures, illustrating the stability of the **G<sub>4</sub>C** crystalline matrix including the superposed **Me<sub>2</sub>1** (cyclamen), **Me<sub>2</sub>2**, or **Me<sub>2</sub>3&Me<sub>2</sub>CBD<sup>S</sup>/CO<sub>2</sub>** complex (blue) and **Me<sub>2</sub>CBD<sup>R</sup>** (orange) photo-products (ball-and-stick); b) crystal structure in stick representation of the **G<sub>4</sub>C{Me<sub>2</sub>1}** complex, which by UV irradiation ( $h\nu$ ) transforms progressively into the **G<sub>4</sub>C{Me<sub>2</sub>2}** and **G<sub>4</sub>C{Me<sub>2</sub>CBD}** host-guest complexes stabilized under confinement by the **G<sub>4</sub>C** host matrix.

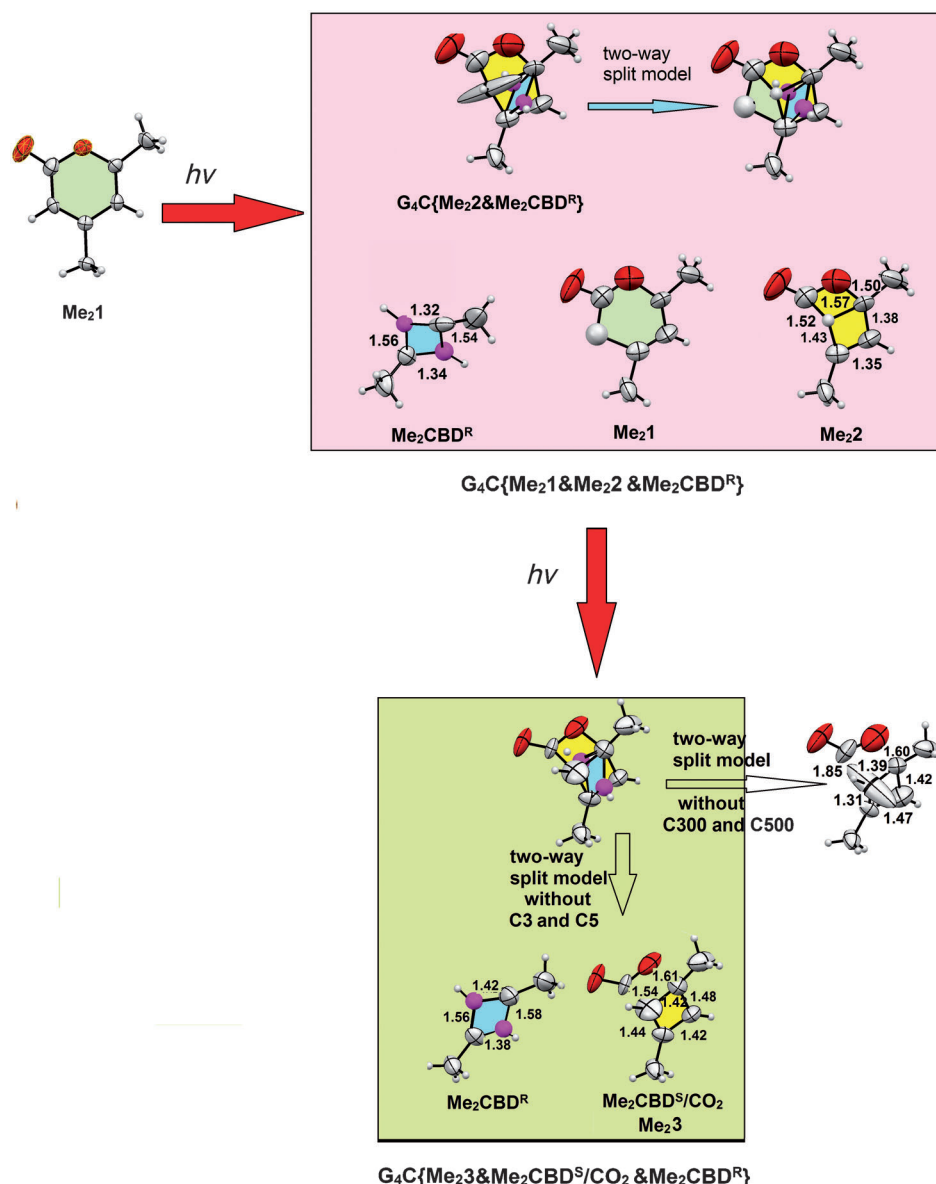


Figure 3. X-ray crystallographic superposed models of the photolysis reaction of 4,6-dimethyl- $\alpha$ -pyrone, **Me<sub>2</sub>1**. Structures are shown for **Me<sub>2</sub>1**, leading after irradiation for 25 min to the Dewar- $\beta$ -lactone **Me<sub>2</sub>2** (77.3%) and the rectangular-bent **Me<sub>2</sub>CBD<sup>R</sup>** (22.7%) and then after irradiation for 60 min to the **Me<sub>2</sub>3&Me<sub>2</sub>CBD<sup>S</sup>/CO<sub>2</sub>** (62.7%) and the rectangular-bent **Me<sub>2</sub>CBD<sup>R</sup>** (37.3%) (see text and Supporting Information for the two-way splitting models).

and the amplification of **Me<sub>2</sub>CBD<sup>R</sup>**. Considering the electron density map of  $G_4C\{Me_23\&Me_2CBD^S/CO_2\&Me_2CBD^R\}$ , which can be connected in a reasonable manner, we may argue that the crystal structure is not really associated with a local disorder (Figure 3). We observe two significant tendencies when **Me<sub>2</sub>2** transforms into **Me<sub>2</sub>3&Me<sub>2</sub>CBD<sup>S</sup>/CO<sub>2</sub>** toward **Me<sub>2</sub>CBD<sup>R</sup>**: 1) the C2–C3 and C6–O1 bonds expand and 2) the C3–C4–C5–C6 ring with a trapezoidal form in **Me<sub>2</sub>2** tends toward a square geometry in **Me<sub>2</sub>CBD<sup>S</sup>** (see the Supporting Information and Figure S1 for details). Owing to a cage and hydrogen-bonding effects, the CO<sub>2</sub> fragment remains close to CBD (Figure 4). Close

inspection of the crystal packing of  $G_4C\{Me_22\}$  reveals an up-down arrangement of **C** molecules in the cone conformation<sup>[27]</sup> that affords free space defined by the internal pocket of component **C**, available to guest molecules during the assembly of the crystal lattice. (Figure 4). In the crystal lattice the bilayer arrangement is consolidated by strong hydrogen bonds between four **G1–G4** cations and eight sulfonate moieties of two **C** molecules.<sup>[28]</sup> The **Me<sub>2</sub>2** molecule is sandwiched between two **G5**, **G6** cations, whereas the carbonyl oxygen atom of **Me<sub>2</sub>2** points outward, forming anchoring hydrogen bonds with a third quasi-coplanar **G7** cation. A last **G8** cation is positioned between two neighboring **C** molecules of the same layer and is perpendicularly oriented to the confined guest molecule (Figure 4). This generates completely closed cavities in the solid state, in which the guest molecules are properly confined through a combination of noncovalent interactions. Under such confined conditions the formation of zwitterion **Me<sub>2</sub>3**<sup>[29]</sup> is more in line with the observed C2–C3 and C6–O1 distances and seems reasonable since the host matrix is ionic/polar (see the Supporting Information for details). The square geometry of the C3–C6 ring is more in line with that of the **Me<sub>2</sub>CBD<sup>S</sup>/CO<sub>2</sub>** complex. These results are similar to the previous theoretical

calculations on energy minima corresponding to distances of 1.6–1.8 Å for the **CBD/CO<sub>2</sub>** complex.<sup>[9]</sup> Moreover, a curious inhibition of the decomposition of the **CBD** has been observed experimentally in the presence of CO<sub>2</sub> in the Ar matrix.<sup>[8]</sup> The most realistic model of the transition-state architecture resulting from the photolysis of **Me<sub>2</sub>2** toward **Me<sub>2</sub>CBD<sup>R</sup>** involves the superposed structures **Me<sub>2</sub>3** and **Me<sub>2</sub>CBD<sup>S</sup>/CO<sub>2</sub>** being present in the  $G_4C$  host matrix. The **Me<sub>2</sub>CBD<sup>R</sup>** rectangular geometry is quantitatively amplified (22.7%  $\rightarrow$  37.3%) after the last irradiation step (Figure 2b). The crystallographic results show that the elimination of CO<sub>2</sub> induces a 90° rotation of the **Me<sub>2</sub>CBD<sup>R</sup>** molecule rela-

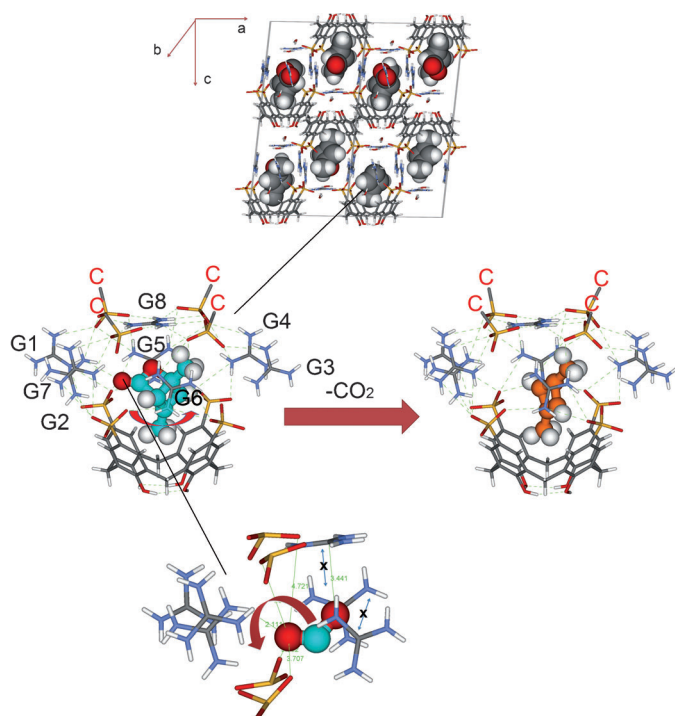


Figure 4. Crystal packing of the  $G_4C[Me_22]$  calixarene bilayers that confine the  $Me_22$  (space-filling representation), and the confined fragmentation of  $Me_22$  to give  $Me_2CBD^R$ .

tive to C3-C4-C5-C6 ring of  $Me_22$  (Figure 3). The -C-H atoms of the cyclobutadiene rings are strongly H-bonded ( $d_{O-H} = 2.83\text{--}2.93 \text{ \AA}$ ) to sulfonate groups, orienting the  $Me_2CBD^R$  and  $Me_2CBD^S$  along the orthogonal diagonals determined by the sulfonate rims.<sup>[18c]</sup>

The  $CO_2$  moiety of  $Me_22$  presents a restricted degree of relative mobility within the host system. A rotational motion toward the  $G7$  moiety might be possible, considering the overall interactions of the  $CO_2$  moiety with the superior/lateral limit of the crystalline matrix. Moreover, one might argue that the  $CO_2$  fragment could not be in such a vicinity with  $Me_2CBD^R$  and therefore is not present in the elementary cells where  $Me_2CBD^R$  is present (see Supporting Information for details)

#### IR and Raman spectroscopic studies in the solid state:

To shed more light on the mechanisms involved in the elimination and the interaction of the  $CO_2$  moiety with cyclobutadiene in confined conditions, we have performed IR (Figure 5) and Raman studies (see Figure S2 in the Supporting Information) on crystalline samples. Close inspection of the

IR spectra shows that the carbonyl vibration bands at  $1710$  and  $1557 \text{ cm}^{-1}$  strongly decrease in intensity at the same rate with irradiation time, whereas a new  $CO_2$ -asymmetric stretching vibration of the  $CO_2$  band at  $2333 \text{ cm}^{-1}$  increases.<sup>[30]</sup> This corresponds to the progressive conversion of the lactone-type compounds  $Me_21$  and  $Me_22$  to  $Me_2CBD^R$  and  $CO_2$ . Krantz et al.<sup>[4]</sup> assumed a face-to-face interaction between  $CBD$  and the bent molecule  $CO_2$ . Our results show that the interaction between  $CO_2$  and the  $CBD$  under confinement is manifested by a shift of about  $17 \text{ cm}^{-1}$  from the position of the free gaseous  $CO_2$  asymmetric fundamental band at  $2350 \text{ cm}^{-1}$ .<sup>[30]</sup>

The absence of the symmetric stretching vibration of the free gaseous  $CO_2$  band at  $2360 \text{ cm}^{-1}$  also shows that the  $CO_2$  is asymmetrically sequestered through hydrogen-bonding and intermolecular interactions with the  $CBD$  within the  $G_4C$  host matrix. Moreover, the absence of these bands in the spectra of the  $G_4C[Me_21]$  and  $G_4C[Me_22]$  host-guest systems is clearly the result of  $CO_2$  development and not because of its simple absorption from air. These IR data leave no doubt that the  $CO_2$  molecule can be considered as a discrete entity during the photochemical process ( $\lambda = 320\text{--}500 \text{ nm}$  at  $175 \text{ K}$ ). Further irradiation with higher energy light,  $\lambda = 190\text{--}500 \text{ nm}$ , does not lead to an important increase of the intensity of the  $CO_2$  vibration band (see Figure 5).

The crystallographic results show that  $Me_2CBD^R$  can be unequivocally identified during the last irradiation step at a maximum conversion of  $37.4\%$  in the presence of the  $Me_23$  and  $Me_2CBD^S/CO_2$  species. It is known that the Dewar- $\beta$ -lactone intermediate gives rise to  $CO_2$  and  $CBD$  when irradiated with light of higher energy ( $\lambda < 290 \text{ nm}$ ).<sup>[2]</sup> It has been shown that the same irradiation energy is also unfavorable for completion of the reaction, since the concentration of  $CBD$  rises to a maximum and then decreases as irradiation is continued, yielding acetylene and  $(CBD)_2$ .<sup>[2]</sup> Unfortunately, only very poor crystals could be obtained by using a high-energy light source ( $\lambda = 190\text{--}500$  at  $175 \text{ K}$ ) and only low intensity data could be collected. The quality of the X-ray diffraction data can only be maintained if the initial irradiation

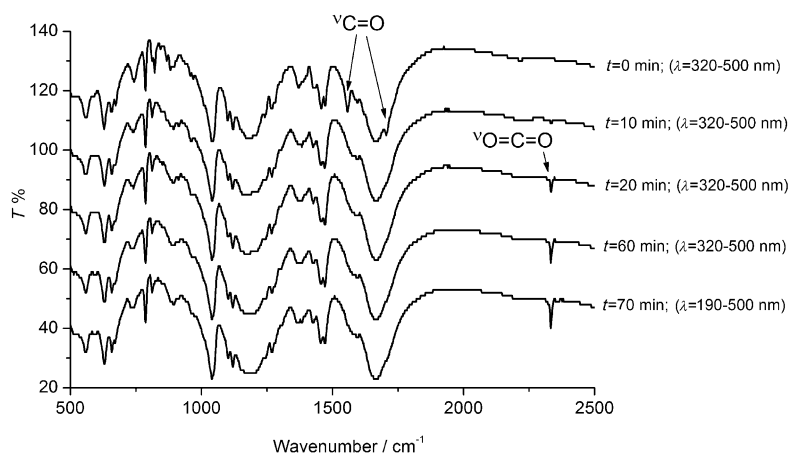


Figure 5. FTIR spectra showing the effect of the irradiation of crystals of  $G_4C[Me_21]$  (black line) at  $\lambda = 320\text{--}500 \text{ nm}$  ( $t = 10, 20, 60 \text{ min.}$ ) and at  $\lambda = 190\text{--}500 \text{ nm}$  ( $t = 70 \text{ min.}$ ).

tion conditions are used:  $\lambda = 320\text{--}500\text{ nm}$ . Moreover the same experiments on the guest matrix  $\mathbf{G}_4\mathbf{C}$  crystals preserve good crystallinity in the absence of the guest molecules. We think that the low-quality X-ray data are related with the critical amount of gaseous  $\text{CO}_2$  developed together with the loss of some of the water molecules induced by local heating during the irradiation. This undermines the matrix integrity and the reaction cannot be completed to isolate  $\text{Me}_2\text{CBD}^{\text{R}}$  as a unique compound in the cavity.

### Synthesis of $\text{Me}_2\text{CBD}$ in aqueous solution under confined conditions:

Following these solid-state studies, the  $\mathbf{G}_4\mathbf{C}\{\text{Me}_2\mathbf{3}\&\text{Me}_2\text{CBD}^{\text{S}}/\text{CO}_2\&\text{Me}_2\text{CBD}^{\text{R}}\}$  crystals obtained after the last irradiation step were dissolved in  $\text{D}_2\text{O}$  and the  $^1\text{H}$  NMR spectrum was recorded. The spectrum shows a series of peaks in a 3:1 ratio, at  $\delta = 1.85\text{--}1.94\text{ ppm}$  and  $\delta = 5.89\text{ ppm}$ , respectively, in accord with experimental<sup>[16]</sup> and theoretical<sup>[31]</sup> reported values for  $\text{CBD}$  (Figure 6a). The mass spectra recorded in  $\text{D}_2\text{O}$  solutions show the correct molecular mass of  $\text{Me}_2\text{CBD}$ : positive-field ionization  $M\text{--D}^+$   $m/z$  82 (Figure 6b) and negative-field ionization,  $M\text{--H}^-$ :  $m/z$  79 (Figure 6c). These measurements are consistent with the major presence of  $\text{Me}_2\text{CBD}$  in aqueous solution, together with other discrete species, which present minor signals.

In general, low-polar organic molecules such as  $\text{Me}_2\mathbf{1}$  or  $\text{Me}_2\text{CBD}$  repel water molecules.<sup>[32]</sup> A special effect can be obtained if molecules with a hydrophilic external hypersurface are available to bind nonpolar substrates in their hydrophobic cavities in solution in water.<sup>[33]</sup> This is the case for  $\text{Me}_2\mathbf{1}$ , which can be solubilized in water in the presence of the  $\mathbf{G}_4\mathbf{C}$  host matrix as the result of the confinement of the  $\text{Me}_2\mathbf{1}$  guest within the calixarene pocket. The  $^1\text{H}$  NMR spectrum of  $\mathbf{G}_4\mathbf{C}\text{--}\{\text{Me}_2\mathbf{1}\}$  features sharp signals, confirming the self-assembly behavior of the host–guest

system previously observed in the solid state: the 4-Me group of  $\text{Me}_2\mathbf{1}$  is hydrophobically confined within the calixarene pocket (see the Supporting Information for details). This assumption was confirmed by the amplified shielding of the  $\text{Me}_4$  hydrogens, by increasing the concentration of the host–guest complex  $\mathbf{G}_4\mathbf{C}\{\text{Me}_2\mathbf{1}\}$  to  $2.5 \times 10^{-2}\text{ mol L}^{-1}$ , and by lowering the temperature from  $25^\circ\text{C}$  to  $7^\circ\text{C}$  (see Figure S4 in the Supporting Information).

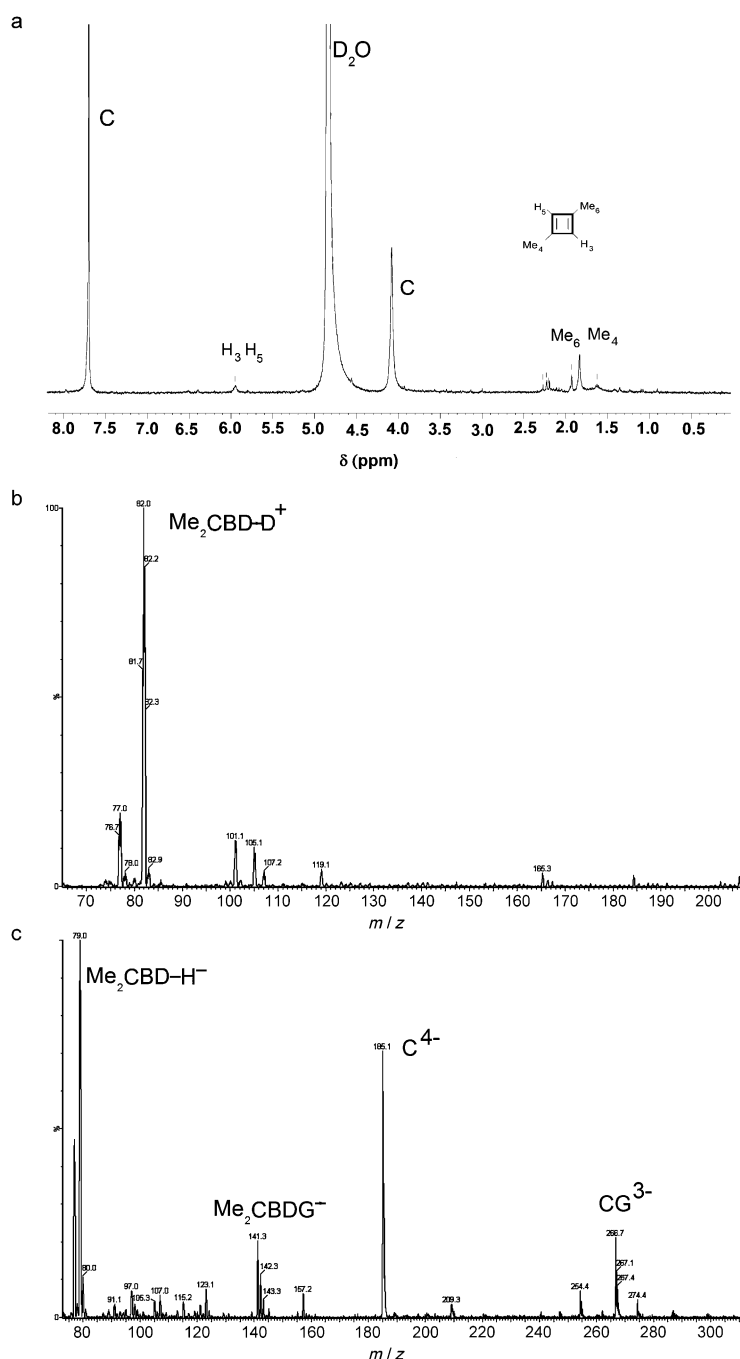


Figure 6. a) 300 MHz  $^1\text{H}$  NMR spectra at  $25^\circ\text{C}$ , b) positive and c) negative electrospray ionization mass spectra of a  $2 \times 10^{-4}\text{ mol L}^{-1}$   $\text{D}_2\text{O}$  solution obtained by dissolving the irradiated crystals of  $\mathbf{G}_4\mathbf{C}\{\text{Me}_2\mathbf{1}\}$  at  $\lambda = 320\text{--}500\text{ nm}$  for 60 min.

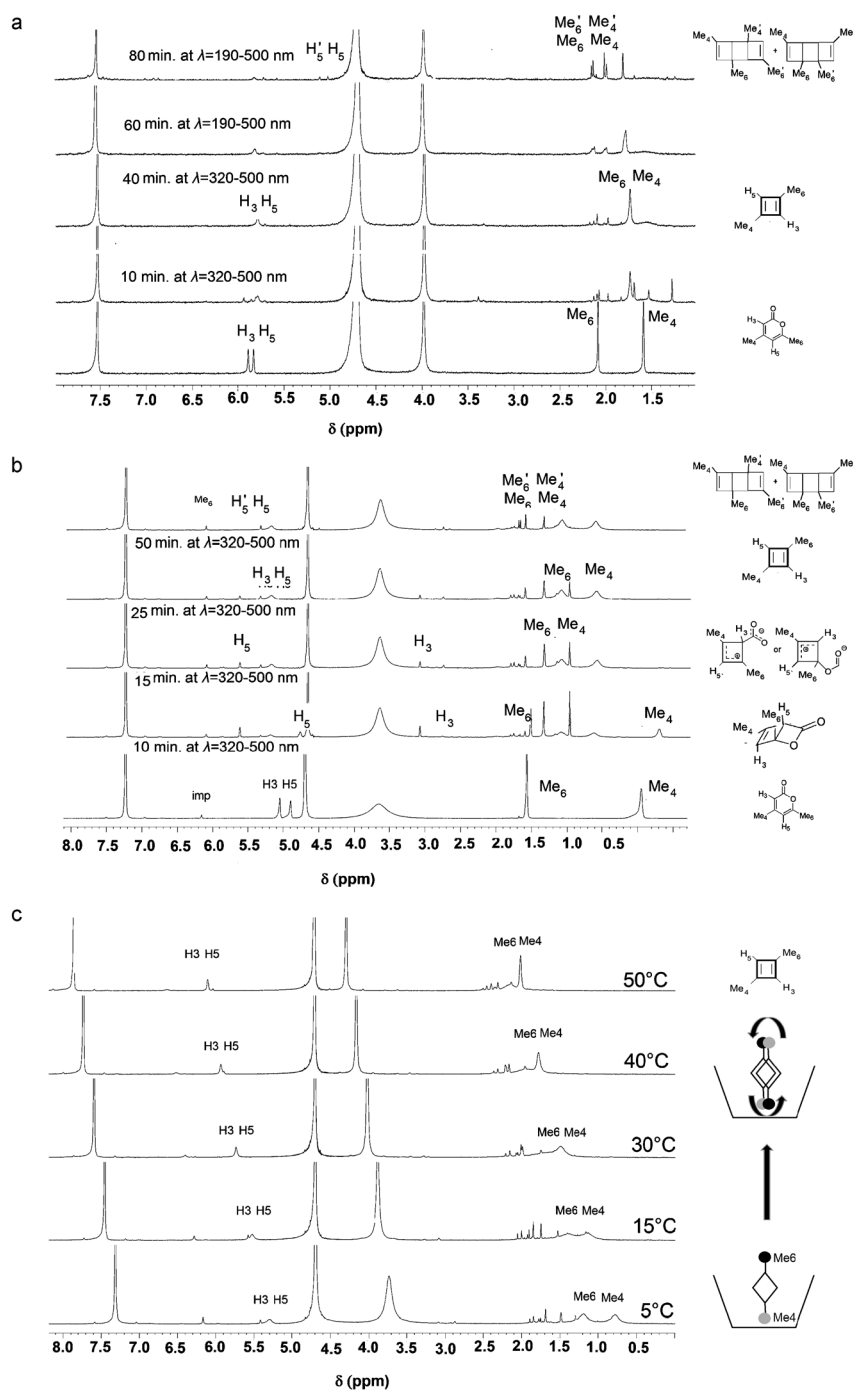


Figure 7. 300 MHz <sup>1</sup>H NMR spectra of the a)  $4.6 \times 10^{-3} \text{ mol L}^{-1}$  and b)  $2.5 \times 10^{-2} \text{ mol L}^{-1}$  D<sub>2</sub>O solutions of **G<sub>4</sub>C[Me<sub>2</sub>1]** at 7 °C for different irradiation times at λ = 320–500 nm or at λ = 190–500 nm; c) 300 MHz <sup>1</sup>H NMR spectra of the  $2.5 \times 10^{-2} \text{ mol L}^{-1}$  D<sub>2</sub>O solution of **G<sub>4</sub>C[Me<sub>2</sub>CBD]** at various temperatures.

Next, the irradiation of a diluted solution of **G<sub>4</sub>C[Me<sub>2</sub>1]** in D<sub>2</sub>O ( $4.6 \times 10^{-3} \text{ mol L}^{-1}$ ) for 10 min at λ = 320–500 nm gave a very complex but sharp <sup>1</sup>H NMR spectrum, indicative of the presence of several discrete species in solution, including the initial **Me<sub>2</sub>1** compound (Figure 7a, second spectrum). After a second irradiation period (30 min) at λ = 320–500 nm, a dramatic simplification of the <sup>1</sup>H NMR spectrum is observed, yielding a series of peaks in an approximately

3:1 ratio, at δ = 1.74 ppm and δ = 5.78 ppm, respectively (Figure 7a, third spectrum). This spectrum is very similar with the <sup>1</sup>H NMR spectrum of dissolved crystals of **G<sub>4</sub>C[Me<sub>2</sub>1]** irradiated at λ = 320–500 nm for 60 min (Figure 6a), and is consistent with the presence of **Me<sub>2</sub>CBD**. As no further apparent alteration in the species distribution was observed on supplementary irradiations at λ = 320–500 nm, further irradiation with higher energy light, λ = 190–500 nm (Figure 7a, third and fourth spectra), led to the progressive conversion of **Me<sub>2</sub>CBD** to its dimers **Me<sub>4</sub>4** and **Me<sub>4</sub>4′**, yielding a series of two new sets of resonances in an approximately 3:1 ratio at δ = 1.98 to 2.15 and; δ = 5.0 to 5.12, respectively.

Having observed important concentration and temperature effects on encapsulation of the **Me<sub>2</sub>1** guest in the **G<sub>4</sub>C** host matrix (see Figure S4 in the Supporting Information for details), we decided to perform the same set of experiments on a more concentrated ( $2.5 \times 10^{-3} \text{ mol L}^{-1}$ ) D<sub>2</sub>O solution of **G<sub>4</sub>C[Me<sub>2</sub>1]** at 7 °C. The <sup>1</sup>H NMR spectra of samples after irradiation at λ = 320–500 nm for 10 and 25 min are consistent with the presence of **Me<sub>2</sub>2**, with signals at δ = 2.75 (H<sub>3</sub>) and 4.80 ppm (H<sub>5</sub>) and δ = 1.48 (Me<sub>6</sub>) and –0.3 ppm (Me<sub>4</sub>) in slow exchange with the carboxyl zwitterions, and **Me<sub>2</sub>3** (Figure 7b), with sharp signals at δ = 3.08 (H<sub>3</sub>) and 5.62 ppm (H<sub>5</sub>) and δ = 1.38 (Me<sub>6</sub>) and 1.03 ppm (Me<sub>4</sub>) (Figure 7b, second and third spectra). These results were confirmed by electrospray mass spectrometry. After the first two irradiation steps at λ = 320–500 nm the initial positive-field ionization of **Me<sub>2</sub>2G<sup>+</sup>** at *m/z* 184 strongly decreases in intensity, whereas a new **Me<sub>2</sub>3GD<sub>2</sub>O<sup>+</sup>** signal at *m/z* 204 increases (see Figure S6 in the Supporting Information). Similarly, the initial negative-field ionizations for **CMe<sub>2</sub>1<sup>4-</sup>** at *m/z* 216 and **CGMe<sub>2</sub>1<sup>3-</sup>** at *m/z* 308 decrease in intensity at the expense of the signals

for  $\text{CMe}_2\text{3D}_2\text{O}^{4-}$  at  $m/z$  220 and  $\text{CGMe}_2\text{3D}_2\text{O}^{3-}$  at  $m/z$  314 (see Figure S7 and S8 in the Supporting Information). These results are consistent with the progressive formation of polar hydrated guest species in the cavity such as  $\text{Me}_2\text{3}^*\text{D}_2\text{O}$  hydrated zwitterions, which seem to be more persistent than low-polar  $\text{Me}_2\text{2}$ , since the host matrix is ionic/polar. Further irradiations at  $\lambda = 320\text{--}500$  nm led to the progressive conversion of  $\text{Me}_2\text{2}$  and  $\text{Me}_2\text{3}$  and the spectrum is consistent with the presence of major amounts of encapsulated  $\text{Me}_2\text{CBD}$ , which displays exchange-broadened signals at  $\delta = 5.20$  (H3,H5) and  $\delta = 1.12$  (Me6) and  $0.67$  (Me4), and minor amounts of the dimers  $\text{Me}_2\text{4}$  and  $\text{Me}_2\text{4}'$  (Figure 7b, fourth, fifth spectra). Importantly, the  $^1\text{H}$  NMR peaks for the methyl hydrogens of  $\text{Me}_2\text{CBD}$  are indicative of methyl groups located in two different magnetic environments (Figure 7b, c). These data demonstrate that high concentrations and lower temperatures increase the stability of  $\text{G}_4\text{C}\{\text{Me}_2\text{CBD}\}$  aggregates based on enhanced hydrophobic effects. To understand the self-assembly phenomena of  $\text{G}_4\text{C}\{\text{Me}_2\text{CBD}\}$  in solution, a variable-temperature NMR study was performed. The two peaks corresponding to  $\text{Me}_2\text{CBD}$  at 278 K converge to give a shielded sharp  $^1\text{H}$  NMR signal at  $\delta = 2.02$  upon heating at 323 K. This suggests that  $\text{Me}_2\text{CBD}$  interconverts rapidly in the calixarene cavity below the coalescence temperature at 313 K (Figure 7c). The H3 and H5 protons initially at  $\delta = 5.30$  ppm converge to give a shielded sharp  $^1\text{H}$  NMR signal at  $\delta = 6.2$  ppm in  $\text{D}_2\text{O}$ . Two levels of diffusion rates were revealed by the NMR DOSY experiments measured under the same conditions (see Figure S5 in the Supporting Information). The  $\text{G}_4\text{C}$  matrix presents a diffusion coefficient of  $2.0 \times 10^{-10} \text{ m}^2 \text{ s}^{-1}$  which is smaller than that of the  $\text{Me}_2\text{CBD}$  molecule ( $3.4 \times 10^{-10} \text{ m}^2 \text{ s}^{-1}$ ) (see Table S1 in the Supporting Information). This indicates that the interconversion process occurs by a releasing process of the  $\text{Me}_2\text{CBD}$  by the cavity of the calixarene in aqueous solution.

The last point we addressed in this study was related to the reversibility of the reaction between  $\text{CBD}$  and  $\text{CO}_2$ , which yields  $\text{Me}_2\text{2}$  or  $\text{Me}_2\text{3}$ . All previous studies agree that the  $\text{CO}_2/\text{CBD}$  interaction results “from the repulsion between  $\text{CBD}$  and  $\text{CO}_2$  rather than an attraction”<sup>[4]</sup> and is mostly favored by the solid matrix constraints/effects.<sup>[1–18]</sup> Within this context, the  $^1\text{H}$  NMR spectra of  $\text{G}_4\text{C}\{\text{Me}_2\text{CBD}\}$  showed no further evolution after the saturation of the aqueous solution with gaseous  $\text{CO}_2$ . These NMR results have been also confirmed by Raman spectroscopy investigations in aqueous solution (see Figure S3 in the Supporting Information for details).

## Conclusion

The present results show that the photolysis reaction of 4,6-dimethyl- $\alpha$ -pyrone,  $\text{Me}_2\text{1}$ , leads to the formation of the dimethyl-Dewar- $\beta$ -lactone  $\text{Me}_2\text{2}$ , the carboxyl zwitterion  $\text{Me}_2\text{3}$ , and 1,3-dimethylcyclobutadiene,  $\text{Me}_2\text{CBD}$ , under hydrophobic confinement in a protective calixarene-guanidini-

um  $\text{G}_4\text{C}$  matrix at lower energetic conditions in the solid crystalline state and in aqueous solution. This is important in the context of efforts by organic chemists to trap cyclobutadiene, to understand its properties, and to elucidate its structure.<sup>[1–14]</sup> However, 4,6-dimethyl- $\alpha$ -pyrone,  $\text{Me}_2\text{1}$ , the dimethyl-Dewar- $\beta$ -lactone  $\text{Me}_2\text{2}$ , and 1,3-dimethylcyclobutadiene,  $\text{Me}_2\text{CBD}$ , have eluded X-ray structural characterization. Our present attempts to isolate the dimethyl-Dewar- $\beta$ -lactone  $\text{Me}_2\text{2}$  and 1,3-dimethylcyclobutadiene in a confined protective crystalline matrix furnish their crystal structures. The geometry of  $\text{Me}_2\text{2}$  is amazingly similar in terms of its bond lengths and angles to that of the Dewar- $\beta$ -lactone molecule predicted by theory.<sup>[12,14]</sup> The crystallographic results show that the elimination of the  $\text{CO}_2$  induces a  $90^\circ$  rotation of the  $\text{Me}_2\text{CBD}^{\text{R}}$  molecule relative to C3-C4-C5-C6 ring of  $\text{Me}_2\text{2}$ . The intermediate structure resulting from the photolysis of  $\text{Me}_2\text{2}$  toward  $\text{Me}_2\text{CBD}^{\text{R}}$  corresponds to a superposition of the  $\text{Me}_2\text{3}$  and  $\text{Me}_2\text{CBD}^{\text{S}}/\text{CO}_2$  structures in the  $\text{G}_4\text{C}$  host matrix. These crystallographic structures are supported by additional FTIR, Raman, and NMR spectroscopic data, and ESI mass spectrometric data from experiments on the photolysis reaction of  $\text{Me}_2\text{1}$  in the solid state and in aqueous solution.

Generations of chemists have considered water for carrying out biological reactions, and only in the last two decades have they shed light on its use as a media to explore the hydrophobic effects in organic reactions.<sup>[32–34]</sup> These considerations inspired us to design unprecedented experiments in which the  $\text{G}_4\text{C}$  system was used as a host protective matrix for the synthesis of  $\text{Me}_2\text{CBD}$  in aqueous solution. Previous or very recent results showed that cyclobutadiene,<sup>[25]</sup> cyclobutadieneiron-tricarbonyl,<sup>[35]</sup> or tetrasilacyclobutadiene<sup>[36]</sup> can be stabilized within a highly protective hydrophobic environment of bulky hydrocarbonous substituents, allowing crystallographic characterization. Herein, of very special interest is the stability of the parent  $\text{Me}_2\text{CBD}$  and its unperturbed precursors  $\text{Me}_2\text{2}$  and  $\text{Me}_2\text{3}$  under protection of the  $\text{G}_4\text{C}$  matrix. Moreover, the  $\text{Me}_2\text{CBD}$  remains stable for several weeks at room temperature and even at  $50^\circ\text{C}$  in aqueous solution. This opens a new perspective for understanding the complex effects that influence the stability of  $\text{Me}_2\text{CBD}$  in aqueous solution. Further research is needed to fully determine the role that water plays in this stabilization and how the protective calixarene-guanidinium  $\text{G}_4\text{C}$  matrix stabilizes such reactive intermediates and products.

## Experimental Section

All the compounds were purchased from Aldrich and used without purification.  $^1\text{H}$  NMR spectra were recorded on an ARX 300 MHz in  $\text{D}_2\text{O}$  with the use of the residual solvent peak as reference. The assignments were made on the basis of COSY and NOESY spectra. Mass spectrometric studies ( $50^\circ\text{C}$ , cone voltage of  $V_c = 5$  V) were performed by using a QuatroMicro triple Quad, Waters apparatus. Samples were introduced directly with a syringe. In situ IR and Raman studies were performed under liquid nitrogen flow or at room temperature by using a Nicolet 710 Apparatus from Thermo Fisher and a Global Source, DTGS detector, re-

spectively, resolution: 4.32 scans and a Labram 1B Confocal from Jobin-Yvon, Ar/Kr Laser 647.1 nm, power 100 mW, detector CCD30-11 1024\*256 pixels, pixel size 26  $\mu\text{m}^2$ , picture area 26.6\*6.7 mm. Optics 50 (numerical opening=0.5), 100 (numerical opening=0.95), Labspec 5 acquisition and treatment software.

**Synthetic procedures: Preparation of  $\text{G}_4\text{C}$ :** The tetra-*p*-sulfocalix[4]arene **C** (0.020 g, 1 equiv) and guanidinium chloride **GCl** (0.010 g, 4 equiv) were dissolved in  $\text{D}_2\text{O}$  (1 mL). After 24 h, colorless single crystals were obtained at room temperature.

**Preparation of  $\text{G}_4\text{C}\{\text{Me}_2\text{I}\}$ :** The tetra-*p*-sulfocalix[4]arene **C** (0.020 g, 1 equiv), guanidine hydrochloride **GCl** (0.010 g, 4 equiv), and 4,6-dimethyl- $\alpha$ -pyrone, **Me<sub>2</sub>I** (0.003 g, 1equiv) were dissolved in  $\text{D}_2\text{O}$  (1 mL). After 17 h, colorless single crystals were obtained at room temperature. High-quality X-ray crystallographic data show the high purity of the crystal formation.<sup>[18]</sup>

**Single-crystal photolysis experiments:** In situ X-ray observation was performed by using single crystals placed on the goniometer, immersed in a  $\text{N}_2$  flow to cool it down to 175 K. The crystal was then, under continuous phi-rotation, irradiated by using a Bluepoint 2.1-UV point source ( $\lambda = 320\text{--}500\text{ nm}$ ). Supplementary ample informative material is provided in the Supporting Information of this paper and in references [17] and [18c] and their Supporting Information. CCDC-764866 and CCDC-764868 contains the supplementary crystallographic data for this paper. These data can be obtained free of charge from The Cambridge Crystallographic Data Centre via [www.ccdc.cam.ac.uk/data\\_request/cif](http://www.ccdc.cam.ac.uk/data_request/cif). The split models discussed in this paper are available as supporting material: CCDC-822948 and CCDC-822949.

**Single-crystal and aqueous solution photolysis experiments:** Single crystals were mixed with KBr to form disk for IR analysis and were used neat for Raman spectroscopic measurements. The samples were immersed in a  $\text{N}_2$  flow to cool them down to 175 K. Single crystals of **CG4** were mixed with 4,6-dimethyl- $\alpha$ -pyrone in water. The complex formed instantaneously and irradiation was carried out directly on aqueous solutions at room temperature.

## Acknowledgements

We thank Simon Parson, Professor of Crystallography at University of Edinburgh, for the crystal structure studies and discussion. This work was supported by funds from the participating organizations of EURYI. see [www.esf.org/euryi](http://www.esf.org/euryi).

- [1] E. J. Corey, J. Streith, *J. Am. Chem. Soc.* **1964**, *86*, 950–951.
- [2] O. L. Chapman, C. L. McIntosh, J. Pacansky, *J. Am. Chem. Soc.* **1973**, *95*, 244–246.
- [3] C. Y. Lin, A. Krantz, *J. Chem. Soc., Chem. Commun.* **1972**, 1111–1112.
- [4] R. G. S. Pong, B. S. Huang, J. Laureni, A. Krantz, *J. Am. Chem. Soc.* **1977**, *99*, 4153–4154.
- [5] G. Maier, *Angew. Chem.* **1974**, *86*, 491–505; *Angew. Chem. Int. Ed. Engl.* **1974**, *13*, 425–438.
- [6] G. Maier, H.-G. Hartan, T. Sayrac, *Angew. Chem.* **1976**, *88*, 252–253; *Angew. Chem. Int. Ed. Engl.* **1976**, *15*, 226–228.

- [7] G. Maier, *Angew. Chem.* **1988**, *100*, 317–341; *Angew. Chem. Int. Ed. Engl.* **1988**, *27*, 309–332.
- [8] B. R. Arnold, J. Michl, *J. Phys. Chem.* **1993**, *97*, 13348–13354.
- [9] K. B. Lipkowitz, R. Larter, *Tetrahedron Lett.* **1978**, *19*, 33–36.
- [10] K. B. Lipkowitz, *J. Am. Chem. Soc.* **1978**, *100*, 7535–7539.
- [11] A. Nemirowski, H. P. Reisenauer, P. R. Screiner, *Chem. Eur. J.* **2006**, *12*, 7411–7420.
- [12] F. Neumann, K. Jug, *J. Org. Chem.* **1994**, *59*, 6437–6441.
- [13] G. Maier, H. P. Reisenauer, *Chem. Ber.* **1981**, 3196–3921.
- [14] S. Breda, L. Lapinski, I. Reva, R. Fausto, *J. Photochem. Photobiol. A* **2004**, *162*, 139–151.
- [15] D. J. Cram, *Angew. Chem.* **1988**, *100*, 1041–1052; *Angew. Chem. Int. Ed. Engl.* **1988**, *27*, 1009–1020.
- [16] D. J. Cram, M. E. Tanner, R. Thomas, *Angew. Chem.* **1991**, *103*, 1048–1051; *Angew. Chem. Int. Ed. Engl.* **1991**, *30*, 1024–1027.
- [17] Y. M. Legrand, A. van der Lee, M. Barboiu, *Science* **2010**, *329*, 299–302.
- [18] a) D. Scheschke, *Science* **2010**, *330*, 1047; b) I. V. Alabugin, B. Gold, M. Shatruk, K. Kovnir, *Science* **2010**, *330*, 1047; c) Y. M. Legrand, A. van der Lee, M. Barboiu, *Science* **2010**, *330*, 1047.
- [19] The parent host structure **G<sub>4</sub>C** and related solvent inclusion structures were independently reported: Y. Liu, M. D. Ward, *Cryst. Growth Des.* **2009**, *9*, 3859–3861.
- [20] M. Brandl, M. S. Weiss, A. Jabs, J. Suhnel, R. Hilgenfeld, *J. Mol. Biol.* **2001**, *307*, 357.
- [21] A. J. Blake, R. O. Gould, S. G. Harris, H. Menab, S. Parsons, *Acta Crystallogr. Sect. C* **1994**, *50*, 1938–1940.
- [22] M. Roeselova, T. Bally, P. Jungwirth, P. Carsky, *Chem. Phys. Lett.* **1995**, *234*, 395–404–410.
- [23] Y. Li, K. N. Houk, *J. Am. Chem. Soc.* **1996**, *118*, 880–885.
- [24] L. T. J. Delbaere, M. N. G. James, N. Nakamura, S. Masamune, *J. Am. Chem. Soc.* **1975**, *97*, 1973–1974.
- [25] S. Masamune, F. A. Souto-Bachiller, T. Machiguchi, J. E. Bertie, *J. Am. Chem. Soc.* **1978**, *100*, 4889–4990.
- [26] D. W. Whitman, B. K. Carpenter, *J. Am. Chem. Soc.* **1980**, *102*, 4272–4274.
- [27] J. L. Atwood, L. J. Barbour, M. J. Hardie, C. L. Raston, *Coord. Chem. Rev.* **2001**, *222*, 3–32, and references therein.
- [28] K. T. Holman, A. M. Pivovar, M. D. Ward, *Science* **2001**, *294*, 1907–1911.
- [29] W. H. Pirkle, L. H. McKendry, *J. Am. Chem. Soc.* **1969**, *91*, 1179–1186.
- [30] G. Socrates, *Infrared and Raman Characteristic Group Frequencies: Tables and Charts*, 3rd ed., Wiley, Chichester, **2001**, p. 142.
- [31] C. Wannere, P. v. R. Schleyer, *Org. Lett.* **2003**, *5*, 605–608.
- [32] R. Breslow, *Acc. Chem. Res.* **1991**, *24*, 159–164.
- [33] R. Breslow, S. D. Dong, *Chem. Rev.* **1998**, *98*, 1997–2011.
- [34] R. N. Butler, A. G. Coyne, *Chem. Rev.* **2010**, *110*, 6302–6337.
- [35] S. Minegishi, K. Komatsu, T. Kitagawa, *Organometallics* **2011**, *30*, 1002–1007.
- [36] a) K. Suzuki, T. Matsuo, D. Hashizume, H. Fueno, K. Tanaka, K. Tamao, *Science* **2011**, *331*, 1306–1309; b) Y. Apeloig, *Science* **2011**, *331*, 1277–1278.

Received: March 5, 2011  
Published online: August 4, 2011